Synoptic-scale controls on the δ^{18}O in precipitation across Beringia

Hannah L. Bailey[1*], Darrell S. Kaufman[2], Andrew C.G. Henderson[1] and Melanie J. Leng[3,4]

[1.] School of Geography Politics & Sociology, Newcastle University, Newcastle upon Tyne, UK.
[2.] School of Earth Sciences and Environmental Sustainability, Northern Arizona University, Flagstaff, AZ 86011, USA.
[3.] NERC Isotope Geosciences Facilities, British Geological Survey, Nottingham, Keyworth, UK.
[4.] Centre for Environmental Geochemistry, School of Geography, University of Nottingham, Nottingham, UK.
[*]Corresponding Author: h.l.bailey@ncl.ac.uk

Abstract

Oxygen isotope records of precipitation ($\delta^{18}O_{precip}$) from Beringia are thought to reflect synoptic-scale circulation changes associated with the Aleutian Low. To delineate the spatial pattern of $\delta^{18}O_{precip}$ associated with the two dominant modes of Aleutian Low circulation, we combine modern $\delta^{18}O_{precip}$ and deuterium excess data with climate reanalysis and back-trajectory modelling. Aleutian Low strength and position are revealed to systematically affect regional moisture source and $\delta^{18}O_{precip}$; whereby a strengthened Aleutian Low causes lower (higher) $\delta^{18}O_{precip}$ in western (eastern) Beringia. We compare a new 100-year-long $\delta^{18}O$ record from the Aleutian Islands with the North Pacific Index, the primary indicator of Aleutian Low strength, and find a significant positive relationship ($r = 0.43$, $p < 0.02$, $n = 28$) that tracks late 20th century change. This study demonstrates synoptic-scale circulation controls on our isotope record, and provides a coherent framework for interpreting existing and emerging paleo-isotope data from the region.

Key Points:

- Isotopes in precipitation track North Pacific pressure-driven circulation
- Oxygen isotope record from Adak correlates with the North Pacific Index
- East-west pressure dipole is exhibited by regional isotope records

1. Introduction

Oxygen isotope records of precipitation ($\delta^{18}O_{precip}$) from Beringia have been shown to reflect changes in atmospheric circulation associated with the Aleutian Low – a large-scale feature of mean low sea-level pressure (SLP) [e.g. *Anderson et al.*, 2005, 2007, 2011; *Fisher et al.*, 2004; *Schiff et al.*, 2009; *Clegg and Hu*, 2010; *Chipman et al.*, 2012; *Jones et al.*, 2014]. As the leading feature of North Pacific climate, this system influences regional temperature and precipitation patterns, including the heat and moisture flux between the extratropical Pacific and Arctic [*Zhu et al.*, 2007]. Collectively, these records are important for assessing the spatio-temporal heterogeneity of climate evolution prior to the instrumental record.

However, most isotope records are located on the eastern edge of this system, and there are discrepancies with interpreting the climate-isotope signal. For example, lower $\delta^{18}O$ in the Mt. Logan ice core [*Fisher et al.*, 2004] and Jellybean Lake record [*Anderson et al.*, 2005] are interpreted as an Aleutian Low intensification, while an isotope-enabled circulation model suggests the opposite [*Field et al.*, 2010]. These inconsistencies call for an observation-based analysis of modern atmospheric processes affecting $\delta^{18}O_{precip}$. This study advances these goals in two ways:

(1) We use the available $\delta^{18}O_{precip}$ data from long-term monitoring stations across Beringia to delineate the spatial pattern of $\delta^{18}O_{precip}$ associated with two contrasting states of Aleutian Low circulation. The resulting pattern provides a framework for interpreting modern and paleo-isotope records in context of regional atmospheric circulation.

(2) We present the first 100-year-long $\delta^{18}O$ record from Adak in the Aleutian Islands, at the heart of the Aleutian Low. Fluctuations in $\delta^{18}O$ are compared with instrumental records and examined in context of the mapped $\delta^{18}O_{precip}$ anomalies, deuterium excess values, and storm-track trajectories. This analysis provides a calibrated approach to interpreting down core

changes in $\delta^{18}O$, and contributes to the growing network of records from this region that is needed to investigate long-term change in atmospheric circulation.

2. Aleutian Low Pressure System

Two distinct patterns of Aleutian Low circulation ('strong' and 'weak') arise from instability in the coupled ocean-atmosphere system [e.g. *Overland et al.*, 1999]. A strong Aleutian Low is defined by a single center of low pressure ~9°E of its mean position (Fig. 1a), and is associated with the eastward expansion of the Asian trough and a stronger North American ridge [*Rodionov et al.*, 2007]. Extratropical cyclones forming east of Japan propagate along a strengthened mid-latitude westerly storm track and pump warm moist air and abundant precipitation into the Gulf of Alaska [*Rodionov et al.*, 2007]. As the Aleutian Low shifts east, the northerly winds that circulate within its northwest quadrant draw polar air to the central and western Aleutian Islands (Fig. 1b). During weak Aleutian Low winters the pressure minimum shifts west and often separates into two centres – one east of Kamchatka and one in the Gulf of Alaska (Fig. 1c) [*Rodionov et al.*, 2007]. The North American ridge shifts to the central North Pacific, effectively blocking the typical west-to-east propagation of cyclones, and storm systems are steered northward over the Aleutian Islands and into the Bering Sea (Fig. 1d) [*Rodionov et al.*, 2007].

These circulation patterns vary on inter-annual to decadal timescales and induce characteristic responses in precipitation, sea surface temperature (SST) and surface air temperature (SAT) [*Mock et al.,* 1998]. Climate anomalies are well expressed in coupled modes of the North Pacific Index (NPI) [*Trenberth and Hurrell*, 1994] and the Pacific Decadal Oscillation (PDO) [*Mantua et al.*, 1997], and are linked to remote El Niño-Southern Oscillation forcing via rossby wave propagation from the tropical Pacific [e.g. *Bjerknes*, 1966; *Trenberth et al.*, 1998]. Specifically, a strong Aleutian Low (−NPI/+PDO) induces positive SSTs, SATs and precipitation anomalies in the Gulf of Alaska and negative

anomalies in the central North Pacific, and the reverse during a weak Aleutian Low

(+NPI/−PDO) [*Mantua et al*., 1997; *Trenberth and Hurrell*, 1994] (Fig. S1 in Supporting

Information). We hypothesize and test how these circulation patterns affect $\delta^{18}O_{precip}$ values

across Beringia through systematic changes in moisture source and storm-track trajectory.

3. Methods

3.1. GNIP $\delta^{18}O$ Data and Back-Trajectory Analysis

Data analyses focus on the region broadly influenced by the Aleutian Low: 155–235°E and

40–75°N. Oxygen and hydrogen isotope precipitation data ($\delta^{18}O_{precip}$ / δD_{precip}) were obtained

from nine stations in the Global Network of Isotopes in Precipitation (GNIP) (Fig. 2a)

[*http://www.iaea.org/water*] and represent composite samples of total precipitation (rain and

snow) accumulated during one calendar month (Table S1, Supporting Information). Monthly

deuterium excess (d-excess) values were calculated as $\delta D - 8.\delta^{18}O$ [*Craig*, 1961], and raw

mean winter (NDJF) $\delta^{18}O_{precip}$ values reduced to precipitation amount-weighted winter values

using the equation:

$$\text{precipitation weighted } \delta^{18}O = \frac{\sum_{i=1}^{n} P_i \delta_i}{\sum_{i=1}^{n} P_i} \tag{1}$$

where P_i and δ_i denote the amount (mm) of each monthly precipitation sample and its

measured oxygen isotope composition, respectively, and n represents the number of months.

The North Pacific Index (NPI) is an instrumental index of Aleutian Low strength calculated

as the area-weighted mean SLP over 30°–65°N and 160°E–140°W [*Trenberth and Hurrell*,

1994]. NPI anomalies were calculated as departures from the 1928−1989 winter mean, and

used to determine whether each winter of GNIP data were characterized by a strong (−NPI)

or weak (+NPI) Aleutian Low. Winter month $\delta^{18}O_{precip}$ values at each GNIP site were

averaged for both Aleutian Low modes, and are presented as anomalies from the long-term

winter mean $\delta^{18}O_{precip}$ for each site.

To spatially interpolate $\delta^{18}O_{precip}$ the data were kriged [Keckler, 1995] using: (a) the long-term winter average $\delta^{18}O_{precip}$ at each GNIP site, and the average $\delta^{18}O_{precip}$ anomalies for (b) strong and (c) weak Aleutian Low winters at each GNIP site (see S1, Supporting Information). Cross-validation was used to quantify the quality of prediction and the spatial distribution of errors within interpolated $\delta^{18}O_{precip}$ values [e.g. Davis, 1987] (Supporting Information S1, Fig. S2). We note interpolated values do not consider smaller-scale geographic parameters influencing $\delta^{18}O_{precip}$ (e.g. orography, temperature) and cannot be considered meaningful across regions with sparse data (e.g. central Alaska). Confidence intervals are greatly reduced in the vicinity of GNIP stations (± 0.10 ‰, 1σ).

Trajectories of precipitating air masses were computed using the Hybrid Single-Particle Lagrangian Integrated Trajectory (HYSPLIT) model [*Draxler and Hess*, 1997]. Gridded hourly NCEP/NCAR meteorological data [*Kalnay et al.*, 1996] were used to calculate daily back-trajectories to Adak for all months of available GNIP $\delta^{18}O_{precip}$ data (1962−67, 1972−1973) on the assumption each trajectory contributed precipitation to the monthly composite $\delta^{18}O_{precip}$ sample. Back-trajectory errors are an estimated 15-30% of the trajectory length, and relate to how well the numerical fields estimate the true flow field in space and time. For full details see Supporting Information S1.

3.2. Sedimentary Analyses

Heart Lake is a small, freshwater through-flow system on Adak Island (51.87°N, 176.63°W). Lake volume is ~8×10^5 m^3 and average outflow is 5×10^4 m^3/day (~15 day retention). Bottom lake water samples were collected for isotope analysis in June 2009 and 2010, with two surface gravity cores (09-AS-1A and 09-AS-1B) from the deepest part of the lake (7.6 m). The upper 12 cm of 09-AS-1B was sampled continuously at 0.5 cm resolution for

radiometric dating (^{210}Pb, ^{226}Ra, ^{137}Cs and ^{241}Am) and both cores were sampled at 0.5 cm resolution for biogenic silica (BSi) and the oxygen isotope composition of diatom silica ($\delta^{18}O_{diatom}$) (see S2 and Table S3 in Supporting Information).

4. Results and Discussion

4.1 Oxygen Isotopes in Precipitation ($\delta^{18}O_{precip}$)

The spatial distribution of mean winter $\delta^{18}O_{precip}$ across Beringia (Fig. 2a) conforms to theoretical and observed understanding; (1) decreasing $\delta^{18}O$ with increasing latitude and elevation [*Dansgaard*, 1964], and (2) decreasing $\delta^{18}O$ with increasing continentality [*Rozanski et al.*, 1993]. For example relatively low $\delta^{18}O_{precip}$ in the Yukon (e.g. Whitehorse winter mean = –24.4 ‰) reflects the cooling and condensing of water vapor as it ascends the coastal mountains and rainout of heavier ^{18}O [e.g. *Dansgaard,* 1964].

Adak mean annual $\delta^{18}O_{precip}$ is –9.00 ‰, while mean winter (DJF) and summer (JJA) values are –10.41 ‰ and –8.40 ‰ respectively. There is no correlation between monthly $\delta^{18}O_{precip}$ and SAT (r = 0.15, n = 72) or precipitation amount (r = 0.03, n = 72). Seasonal $\delta^{18}O_{precip}$ differences (±2.01 ‰) broadly reflect progressive loss of ^{18}O in water vapor during the poleward transport and condensation of marine air masses from the mid-latitudes to Adak during winter, leading to a climatological decrease of $\delta^{18}O$ in vapor (and thereby precipitation) with temperature [e.g. *Dansgaard*, 1964].

The spatial distribution of mean $\delta^{18}O_{precip}$ during strong and weak Aleutian Low winters are presented as departures from the long-term winter means (Fig. 2b, 2c). During a strong Aleutian Low, winter $\delta^{18}O_{precip}$ anomalies exhibit a dipole pattern over western Alaska (negative) and the Yukon (positive) (Fig. 2b). Higher $\delta^{18}O_{precip}$ in the Yukon can be attributed to enhanced cyclonic circulation and meridional flow delivering warm moist Pacific air enriched in ^{18}O (Fig. 1b), consistent with modelled $\delta^{18}O_{precip}$ output by *Field et al.* [2010].

The spatial $\delta^{18}O_{precip}$ pattern during a weak Aleutian Low demonstrates the opposite: higher $\delta^{18}O_{precip}$ in western Alaska and lower $\delta^{18}O_{precip}$ in the Yukon and Kamchatka (Fig. 2c). Differences between strong and weak Aleutian Low $\delta^{18}O_{precip}$ values are significant ($p < 0.05$) and greatly exceed interpolation error (Fig. S2).

Barrow $\delta^{18}O_{precip}$ anomalies highlight the sensitivity of Arctic Alaska to North Pacific circulation patterns, which likely relates to latitudinal migration of the polar front. Persistent winter sea ice implies a distal moisture source; hence, a 52% increase in total precipitation during a weak Aleutian Low [data available at: *http://www.ncdc.noaa.gov*] can be attributed to an enhanced southerly moisture flux and transport of ^{18}O-enriched vapor. Alternatively, air-mass trajectories cross the Arctic Ocean during a strong Aleutian Low, where the prevalence of sea ice, high aridity, and lower temperatures account for lower $\delta^{18}O_{precip}$ and a reduction in total precipitation (data not shown).

4.2. Processes Controlling $\delta^{18}O_{precip}$ on Adak Island

Mean winter $\delta^{18}O_{precip}$ is significantly ($p < 0.05$) lower on Adak during a strong Aleutian Low (−1.14 ‰, n = 14) compared to a weak Aleutian Low (+0.44 ‰, n = 7) (Fig. 2b, c). Furthermore, Adak monthly back-trajectories indicate systematic differences in air-mass source and trajectory. During a strong Aleutian Low, back-trajectories at 48hrs originate in the north and span an area from 48–85 °N and 154–230 °E (Fig. 2b), and during a weak Aleutian Low, back-trajectories at 48hrs originate in the west/south-west and span an area from 29–65 °N and 140–200 °E (Fig. 2c).

We propose changes in the strength and position of the Aleutian Low shift the moisture source location for precipitation falling at Adak and across Beringia. When the SLP minimum is near Adak (strong Aleutian Low), precipitating air masses from the north bring vapor and precipitation relatively depleted in ^{18}O (Fig. 1b, Fig. 2b), as well as lower-than-

average winter temperatures (−0.5 °C) and increased snowfall (> 556 mm). Unlike liquid precipitation, snow (and other solid precipitation) will not equilibrate with ambient moisture by continuous exchange during the descent from cloud-base to the ground [*Dansgaard*, 1964], and hence any moisture source 'effects' will be retained.

Alternatively, increased temperatures and rainfall (> 148 mm) during a weak Aleutian Low reflects more prevalent south-westerly storm tracks (Fig. 1D) [e.g. *Rodionov et al.*, 2007]. These storms carry warm ^{18}O-enriched vapor to Adak from as south as 29 °N (48 hrs prior) (Fig. 2c, and Fig. S3 in Supporting Information). Precipitation has relatively high $\delta^{18}O$ values, and these are likely amplified by post-condensational exchange with the ambient moisture as it falls to the ground [e.g. *Dansgaard*, 1964; *Pfahl et al.*, 2012].

4.3 Deuterium Excess and Moisture Source

Deuterium excess (d-excess; [*Craig*, 1961]) is determined by evaporative conditions of the source region (e.g. relative humidity, SST) [see *Pfahl and Sodemann*, 2014], as well as kinetic processes during vapor transport and condensation (e.g. ice-crystal formation, re-evaporation) [*Dansgaard*, 1964; *Jouzel and Merlivat*, 1984; Gat, 1996]. Adak winter month d-excess and $\delta^{18}O_{precip}$ negatively correlate (r = −0.56, p < 0.01, n = 48) (Fig. 3), and HYSPLIT output shows d-excess values of Arctic-derived precipitation (+9.6 ‰) are significantly (p < 0.01) higher than Pacific-derived (+4.6 ‰). These differences reflect the slower diffusivity of $H_2^{18}O$ relative to HDO during evaporation above the ocean surface [*Dansgaard*, 1964]. Specifically, high d-excess values arise when there is insufficient time for vapour to equilibrate between the saturated ocean surface layer and the sub-saturated atmosphere [e.g. *Pfahl and Sodemann*, 2014]. Evaporated moisture entrained in the Arctic (as opposed to Pacific) is subject to such conditions, whereby large humidity gradients between the ocean surface and the dry atmosphere above − particularly at the sea ice margin [e.g. *Kurita*, 2011] – will lead to strong non-equilibrium (kinetic) fractionation and an evaporate

characterized by relatively high d-excess and low $\delta^{18}O$ [e.g. *Gat et al.*, 2003; *Uemura et al.*, 2008; *Pfahl and Sodemann*, 2014]. Furthermore, Adak receives increased snowfall during months with Arctic-derived moisture, and this will also be characterized by high d-excess due to non-equilibrium condensation during ice particle growth [*Jouzel and Merlivat*, 1984].

4.4 Paleo-Records of $\delta^{18}O_{precip}$ and Atmospheric Circulation

4.4.1. Heart Lake Aleutian Low Proxy Record

We use our $\delta^{18}O_{diatom}$ record from Adak to determine whether changes in the Aleutian Low are captured in natural archives of $\delta^{18}O_{precip}$. Diatom silica is thought to precipitate in isotopic equilibrium with the surrounding water, and therefore $\delta^{18}O_{diatom}$ resembles the $\delta^{18}O$ of the lake water ($\delta^{18}O_{LW}$) in which the diatom grows at a specific temperature [*Leng and Barker*, 2006]. Heart Lake is a through-flow system with short retention (~15 days) and its primary component is precipitation it receives directly, and indirectly through surface water runoff and groundwater input. Accordingly, Heart Lake $\delta^{18}O_{LW}$ resembles measured $\delta^{18}O_{precip}$ at Adak (Fig. S6, Supporting Information). Previous diatom and $\delta^{18}O_{diatom}$ analyses in Heart Lake rule out potential disequilibrium effects [*Bailey et al.*, 2014]; hence $\delta^{18}O_{diatom}$ should reflect $\delta^{18}O_{precip}$ changes associated with the Aleutian Low.

The North Pacific Index (NPI) is a direct instrumental index of Aleutian Low strength [*Trenberth and Hurrell*, 1994]. Each 0.25-cm-thick sample analyzed for $\delta^{18}O_{diatom}$ represents approximately 1−5 years, so our $\delta^{18}O_{diatom}$ time series is compared with the 5-year running mean of winter NPI values (monthly NPI values averaged over November−February) from 1900 to 2009. We use winter NPI values because in late spring, when the main diatom bloom occurs [*Bailey et al.*, 2014], we estimate winter snowpack melt exceeds spring precipitation input. This estimate is based on local long-term (1942−1997) mean March snow depths (250 mm) which, assuming uniform snow distribution across the catchment (8 km^2) and a mean density of 250 kg/m^3 for settled snow [*Cuffey and Paterson*, 2010], equate to ~5 x 10^5 m^3

water equivalent entering Heart Lake during the spring melt. This volume exceeds spring precipitation inputs ($\sim 4 \times 10^5$ m^3), hence Heart Lake spring $\delta^{18}O_{LW}$ values will trend toward winter $\delta^{18}O_{precip}$ values [e.g. *Kortelainen and Karhu*, 2004; *Jonsson et al.*, 2009]. This is evidenced by Heart Lake $\delta^{18}O_{LW}$ samples taken in June (mean = −9.5 ‰) which are more comparable to mean January (−9.3 ‰) than mean June (−8.1 ‰) $\delta^{18}O_{precip}$ values.

Heart Lake $\delta^{18}O_{diatom}$ and the NPI correlate significantly; r = 0.43, p < 0.02, n = 28, whereby a stronger Aleutian Low (–NPI) corresponds with lower $\delta^{18}O_{diatom}$ (Fig. 4). Adjustment for autocorrelation does not increase the p-value. There is no correlation between $\delta^{18}O_{diatom}$ and the spring/summer NPI over the same 1900−2009 period (r = 0.09, p < 0.60, n = 28). The $\delta^{18}O_{diatom}$ values from Heart Lake vary between +27.3 and +30.3 ‰ ($\overline{x}$ = +29.11 ‰) and gradually decrease over the past century [e.g. *Trenberth and Hurrell,* 1994]. Weak positive correlations between $\delta^{18}O_{diatom}$ and mean winter temperature (r = 0.14, p < 0.60, n = 19) and precipitation (r = 0.10, p < 0.70, n = 19) are consistent with measured NPI climate anomalies on Adak Island (see Fig. S1), though are insignificant. A stronger relation between $\delta^{18}O_{diatom}$ and the winter surface pressure field (r = 0.43) indicates the dominant controls on $\delta^{18}O_{diatom}$ are the effects of water vapor origin and transport path (Fig. 2a,b).

4.4.2. Comparison with Regional Aleutian Low Records

Comparison of existing isotope records from Beringia shows an opposite west-east relation with the winter NPI over the past 100 years (Fig. 5). Our western $\delta^{18}O$ record from Heart Lake positively correlates with the NPI (r = 0.43, p < 0.02, n =28); while eastern records Jellybean Lake (r = −0.48, p < 0.02, n = 24) [*Anderson et al.*, 2005] and Mt. Logan (r = −0.10, p < 0.20, n = 101) [*Moore et al.*, 2002] negatively correlate with the NPI. This dipole-like pattern corresponds to the mapped GNIP $\delta^{18}O_{precip}$ anomalies (Fig. 2a, 2b). The 100-year $\delta^{18}O_{diatom}$ record from Heart Lake is also consistent with other NPI-inferred paleo-records

from across Beringia, including northwest North American tree-ring records (r = 0.66, p < 0.001) [*D'Arrigio et al.*, 2005], Na+ concentrations in Mt. Logan ice (r = −0.45, p < 0.001) [*Osterberg et al.*, 2014], and the weight abundance of BSi in Heart lake (r = −0.48, p < 0.01) [*Krawiec and Kaufman*, 2014].

Raw $\delta^{18}O_{calcite}$ data from Jellybean Lake [*Anderson et al.*, 2005] [available from: *http://www.ncdc.noaa.gov*] negatively correlate with the NPI over the 100-year instrumental period (r = −0.48, p < 0.02) (Fig. 5d), though the inverse correlation (r = 0.48) is stated in *Anderson et al*. [2005]. Our revised calculation is supported by the mapped GNIP $\delta^{18}O_{precip}$ anomalies (Fig. 2), and by *Field et al*. [2010] whose isotope-enabled GCM simulates higher $\delta^{18}O_{precip}$ around the Gulf of Alaska during a strengthened Aleutian Low.

5. Conclusions

We demonstrate a west-east dipole pattern in $\delta^{18}O_{precip}$ associated with synoptic-scale atmospheric circulation over the North Pacific. Analyses of $\delta^{18}O_{precip}$ reveal the dominant effect of a strengthened Aleutian Low is higher (lower) $\delta^{18}O_{precip}$ in the east (west), and this can be attributed to water vapor origin and moisture trajectory. This new $\delta^{18}O$ record from sedimentary diatoms in Heart Lake demonstrates their ability to capture changes in synoptic-scale atmospheric circulation. Furthermore, our interpolation scheme demonstrates the paucity of $\delta^{18}O_{precip}$ data across Beringia and highlights target areas for future sampling.

Acknowledgments

References

Anderson, L., M. B. Abbot, B. P. Finney, and S. J. Burns (2005), Regional atmospheric

circulation change in the North Pacific during the Holocene inferred from lacustrine

carbonate oxygen isotopes, Yukon Territory, Canada, *Quat. Res*., **64**, 21–35, doi:

10.1016/j.yqres.2005.03.005.

Anderson, L., M. B. Abbot, B. P. Finney, and S. J. Burns (2007), Late Holocene moisture

balance variability in the southwest Yukon Territory, Canada, *Quat. Sci. Rev*., **26**, 130–141,

doi: 10.1016/j.quascirev.2006.04.011.

Anderson, L., B. P. Finney, and M. D. Shapley (2011), Lake carbonate δ^{18}O-records from the

Yukon Territory, Canada: Little Ice Age moisture variability and patterns, *Quat. Sci. Rev*., **30**,

887–898, doi: 10.1016/j.quascirev.2011.01.005.

Bailey, H. L., A. C. G. Henderson, H. J. Sloane, A. Snelling, M. J. Leng, and D. S. Kaufman

(2014), The effect of species on lacustrine δ^{18}O$_{diatom}$ and its implications for

paleoenvironmental reconstructions, *J. Quaternary Sci*., **29**, 393–400, doi: 10.1002/jqs.2711.

Bjerknes, J. (1966), A possible response of the atmospheric Hadley circulation to equatorial

anomalies of the ocean temperature, *Tellus,* **18,** 820–829, doi: 10.1111/j.2153-3490.1966.tb00303.x.

Chipman, M. C., B. F. Clegg, and F. S. Hu (2012), Variation in the moisture regime of northeastern interior Alaska and possible linkages to the Aleutian Low: Inferences from a late-Holocene δ^{18}O record, *J. Paleolimnol.*, **48**, 69–81, doi: 10.1007/s10933-012-9599-0.

Clegg, B. F., and F. S. Hu (2010), An oxygen-isotope record of Holocene climate change in south-central Brooks Range, Alaska, *Quat. Sci. Rev.*, **29**, 928–939, doi: 10.1016/j.quascirev.2009.12.009.

Coplen, T. B., P. J. Neiman, A. B. White, J. M. Landwehr, F. M. Ralph, and M. D. Dettinger (2008), Extreme changes in stable hydrogen isotopes and precipitation characteristics in a landfalling Pacific storm, *Geophys. Res. Lett.*, **35**, L21808, doi:10.1029/2008GL035481.

Craig, H. (1961), Isotopic variations in meteoric waters, *Science*, **133**, 1702–1703, doi: 10.1126/science.133.3465.1702.

Cuffey, K. M., and W. S. B. Paterson (2010), The Physics of Glaciers, Fourth Edition, Elsevier, Oxford.

Davis, B. M. (1987), Uses and abuses of cross-validation in geostatistics, *Math. Geol.*, 19, 241–248, doi: 10.1007/BF00897749.

D'Arrigo, R., R. Wilson, C. Deser, G. Wiles, E. Cook, R. Villalba, A. Tudhope, J. Cole, and B. Linsley (2005), Tropical-North Pacific climate linkages over the past four centuries, *J. Clim.*, **18**(24), 5253–5265, doi:10.1175/jcli3602.1.

Dansgaard, W. (1964), Stable isotopes in precipitation, *Tellus*, **16**, 436–468, doi:10.1111/j.2153-3490.1964.tb00181.x.

Draxler, R. R., and G. D. Hess (1997), An overview of the HYSPLIT_4 modeling system for trajectories, dispersion and deposition, *Aust. Meteorol. Mag.*, **47**, 295–308.

Draxler, R.R. and Rolph, G.D. (2015) HYSPLIT (Hybrid Single-particle Lagrangian Integrated Trajectory) Model access via NOAA ARL READY Website (http://ready.arl.noaa.gov/HYSPLIT.php). NOAA Air Resources Laboratory, Silver Spring, MD.

Ersek, V., A. C. Mix, and P. U. Clark (2010), Variations of δ^{18}O in rainwater from southwestern Oregon, *J. Geophys. Res.*, **115**, D09109, doi:10.1029/2009JD013345.

Field, R. D., G. W. K. Moore, G. Holdsworth, and G. A. Schmidt (2010), A GCM‐based analysis of circulation controls on δ^{18}O in the southwest Yukon, Canada: Implications for climate reconstructions in the region, *Geophys. Res. Lett.*, **37**, L05706, doi:10.1029/2009GL041408.

Fisher, D. A., C. Wake, K. Kreutz, K. Yalcin, E. Steig, P. Mayewski, L. Anderson, J. Zheng, S. Rupper, C. Zdanowicz, M. Demuth, M. Waszkiewicz, D. Dahl-Jensen, K. Goto-Azuma, J. B. Bourgeois, R. M. Koerner, J. Sekerka, E. Osterberg, M. B. Abbott, B. P. Finney, and S. J.

Burn (2004), Stable isotope records from Mount Logan, Eclipse ice cores and nearby Jellybean Lake. Water cycle of the North Pacific over 2000 years and over five vertical kilometres: Sudden shifts and tropical connections, *Geogr. Phys. Quat.*, **58** (2–3), 337–352, doi: 10.7202/013147ar.

Gat, J. (1996), Oxygen and hydrogen isotopes in the hydrological cycle, *Annu. Rev. Earth Planet. Sci.*, **24**, 225–262, doi: 10.1146/annurev.earth.24.1.225.

Gat, J. R., B. Klein, Y. Kushnir, W. Roether, H. Wernli, R. Yam, and A. Shemesh (2003), Isotope composition of air moisture over the Mediterranean Sea: an index of the air-sea interaction pattern, *Tellus B*, **55**, 953–965, doi: 10.1034/j.1600-0889.2003.00081.x.

Jones, M. C., M. Wooller, and D.M. Peteet (2014), A deglacial and Holocene record of climate variability in south-central Alaska from stable oxygen isotopes and plant macrofossils in peat, *Quat. Sci. Rev.*, **87**, 1–11, doi: 10.1016/j.quascirev.2013.12.025.

Jonsson, C. E., M. J. Leng, G. C. Rosqvist, J. Seibert, and C. Arrowsmith (2009), Stable oxygen and hydrogen isotopes in sub-Arctic lake waters from northern Sweden, *J. Hydrol.*, **376**, 143–151, doi: 10.1016/j.jhydrol.2009.07.021.

Jouzel, J., and L. Merlivat (1984), Deuterium and oxygen 18 in precipitation: Modeling of the isotopic effects during snow formation, *J. Geophys. Res.*, **89**(D7), 11749–11757, doi:10.1029/JD089iD07p11749.

Kalnay, E., M. Kanamitsu, R. Kistler, W. Collins, D. Deaven, L. Gandin, M. Iredell, S. Saha, G. White, J. Woollen, Y. Zhu, A. Leetmaa, R. Reynolds, M. Chelliah, W. Ebisuzaki, W.

Higgins, J. Janowiak, K. C. Mo, C. Ropelewski, J. Wang, Roy Jenne, and D. Joseph (1996), The NCEP/NCAR 40-Year Reanalysis Project, *Bull. Amer. Meteor. Soc.*, **77**, 437–471, doi: 10.1175/1520-0477(1996)077<0437:TNYRP>2.0.CO;2.

Keckler, D. (1995) The Surfer Manual. Golden, CO.: Golden Software, Inc.

Kortelainen, N. M., and J. A. Karhu (2004), Regional and seasonal trends in the oxygen and hydrogen isotope ratios of Finnish groundwaters: a key for mean annual precipitation. *J. Hydrol.*, **285**, 143–157, doi:10.1016/j.jhydrol.2003.08.014.

Krawiec, A. C. L., and D. S. Kaufman (2014), Holocene storminess inferred from sediments of two lakes on Adak Island, Alaska, *Quat. Res.,* **82**, 73–84, doi: 10.1016/j.yqres.2014.02.007.

Kurita, N. (2011), Origin of Arctic water vapor during the ice‐growth season, *Geophys. Res. Lett.*, **38**, L02709, doi:10.1029/2010GL046064.

Leng, M. J., and Barker, P. A. (2006), A review of the oxygen isotope composition of lacustrine diatom silica for palaeoclimate reconstruction, *Earth. Sci. Rev*, **75**, 5–27, doi: 10.1016/j.earscirev.2005.10.001.

Mantua, N. J., S. R. Hare, Y. Zhang, J. M. Wallace, and R. C. Francis (1997), A Pacific interdecadal climate oscillation with impacts on salmon production, *Bull. Am. Meteorol. Soc.*, **78**, 1069–1079, doi: 10.1175/1520-0477(1997)078<1069:APICOW>2.0.CO;2.

Mock, C. J., P. J. Bartlein, and P. M. Anderson (1998), Atmospheric circulation patterns and

spatial climatic variations in Beringa, *Internat. J. Climatol.,* **10**, 1085–1104, doi:
10.1002/(SICI)1097-0088(199808)18:10<1085::AID-JOC305>3.0.CO;2-K.

Moore, G.W.K., G. Holdsworth, and K. Alverson (2002), Mount Logan Ice Core Isotope and
Accumulation Data, IGBP PAGES/World Data Center for Paleoclimatology Data
Contribution Series #2002-79. NOAA/NCDC Paleoclimatology Program, Boulder CO, USA.

Osterberg, E.C., P. A. Mayewski, D.A. Fisher, K. J. Kreutz, K. A. Maasch, S. B. Sneed, and
E. Kelsey (2014), Mount Logan ice core record of tropical and solar influences on Aleutian
Low variability: 500–1998 A.D., *J. Geophys. Res. Atmos*., **119**, 11,189–11,204,
doi:10.1002/2014JD021847.

Overland, J. E., J. M. Adams, and N. A. Bond (1999), Decadal variability of the Aleutian
Low and its relation to high-latitude circulation, *J.Clim.*, **12**, 1542–1548, doi: 10.1175/1520-
0442(1999)012<1542:DVOTAL>2.0.CO;2.

Pfahl, S., and H. Sodemann (2014), What controls deuterium excess in global precipitation?,
Clim. Past., **10**, 771−781, doi: 10.5194/cp-10-771-2014.

Pfahl, S., H. Wernli, and K. Yoshimura (2012), The isotopic composition of precipitation
from a winter storm – a case study with the limited-area model COSMOiso, *Atmos. Chem.
Phys.*, **12**, 1629−1648, doi: 10.5194/acp-12-1629-2012.

Rodionov, S. N., N. A. Bond, and J. E. Overland (2007), The Aleutian Low, storm tracks, and
winter climate variability in the Bering Sea, *Deep Sea Res.II*., **54**, 2560–2577, doi:

10.1016/j.dsr2.2007.08.002.

Rozanski, K., L. Araguás-Araguás, and R. Gonfiantini (1993), Isotopic patterns in modern global precipitation, in Climate Change in Continental Isotopic Records, *Geophys. Monogr. Ser.*, vol 78, edited by P. K. Swart et al., pp. 1−36, AGU, Washington, D.C.

Schiff, C. J., D. S. Kaufman, A. P. Wolfe, J. Dodd, and Z. Sharp (2009), Late Holocene storm-trajectory changes inferred from the oxygen isotope composition of lake diatoms, south Alaska, *J. Paleolimnol.*, **41**, 189–208, doi: 10.1007/s10933-008-9261-z.

Trenberth, K. E., and J. W. Hurrell (1994), Decadal atmosphere-ocean variations in the Pacific, *Clim. Dyn.*, **9**, 303–319, doi: 10.1007/BF00204745.

Trenberth, K. E., G.W. Branstator, D. Karoly, A. Kumar, N.-C. Lau, and C. Ropelewski (1998), Progress during TOGA in understanding and modeling global teleconnections associated with tropical sea surface temperatures, J. Geophys. Res., **103**(C7), 14,291–14,324, doi:10.1029/97JC01444.

Uemura, R., Y. Matsui, K. Yoshimura, H. Motoyama, and N. Yoshida (2008), Evidence of deuterium excess in water vapor as an indicator of ocean surface conditions, *J. Geophys. Res.*, **113**, D19114, doi:10.1029/2008JD010209.

Zhu, X., J. Sun., Z. Liu, Q. Liu, and J. E. Martin (2007), A synoptic analysis of the interannual variability of winter cyclone activity in the Aleutian Low region, *J. Clim*, **20**, 1523–1538, doi: 10.1175/JCLI4077.1.
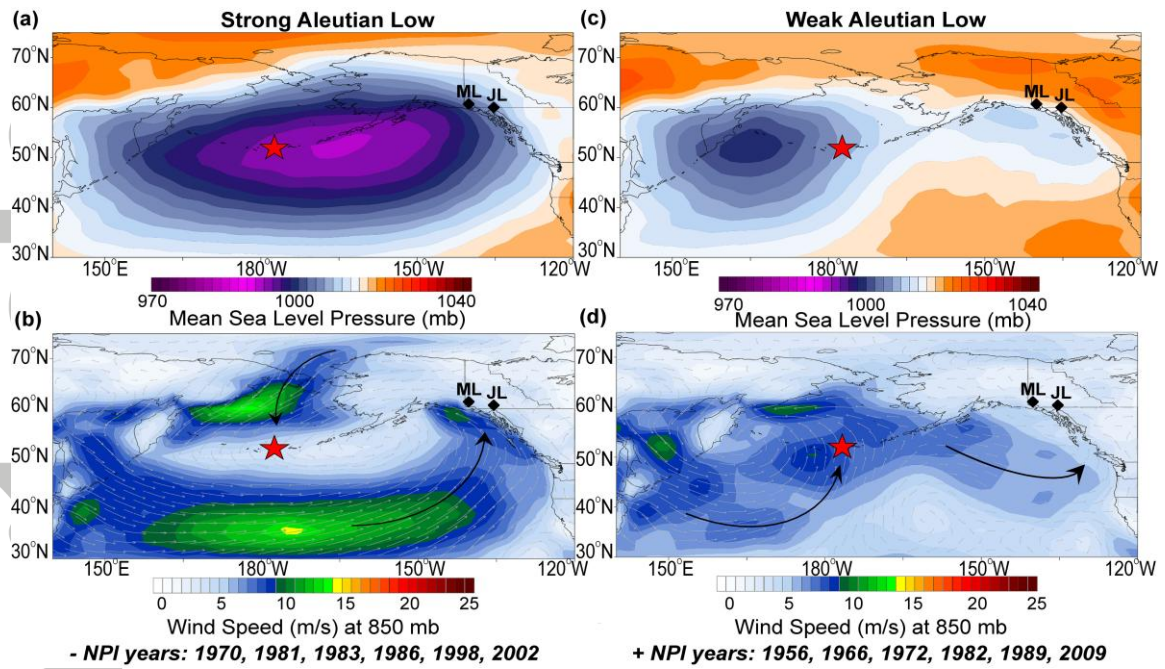
Figure 1. Mean winter (NDJF) sea level pressure and wind fields associated with the six most negative (a, b) and positive (c, d) North Pacific Index (NPI) values between 1950-2014 [*Trenberth and Hurrell*, 1994]. A negative (positive) NPI is a strong (weak) Aleutian Low. Heart Lake is marked by a star; black diamonds indicate Mt. Logan (ML) and Jellybean Lake (JL). Black arrows highlight the main storm tracks. Data obtained from NCEP/NCAR V1 reanalysis [*Kalnay et al.*, 1996].
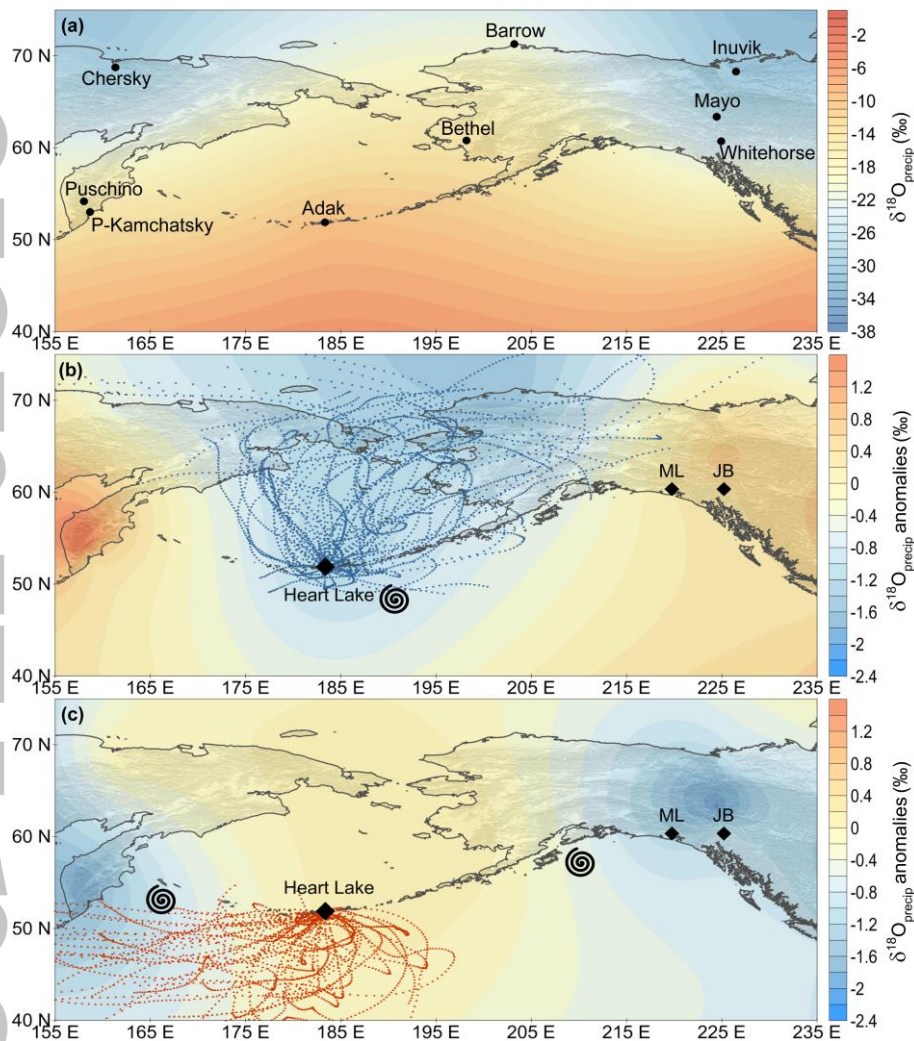
Figure 2. Mean winter $\delta^{18}O_{precip}$ and back-trajectories for (a) 1960-2009 (b) strong, and (c) weak Aleutian Low winters. Values in b and c are expressed as anomalies from the long-term winter mean for each GNIP site (circle). Spirals mark mean Aleutian Low positions, dotted curves plot the mean moisture trajectories during strong (blue) and weak (red) Aleutian Low circulation during the corresponding months, and were modelled using HYSPLIT [*Draxler and Hess*, 1997]. Dots represent hourly intervals along each trajectory. Sites referred to in text are marked by diamonds: Heart Lake, Mt. Logan (ML) and Jellybean Lake (JL). Data and all trajectories are listed in Table S1 and Figure S2 in Supporting Information.
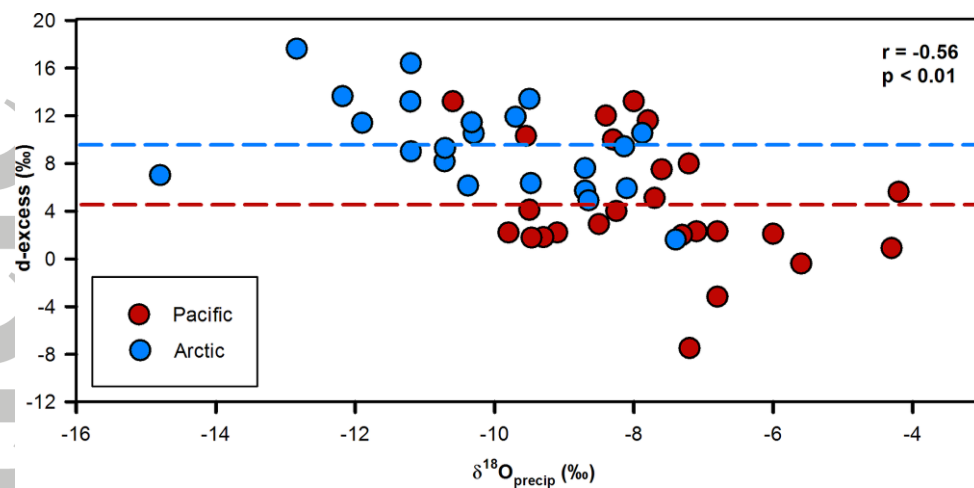
Figure 3. Winter month d-excess and $\delta^{18}O_{precip}$ values for Adak precipitation (1960-1973). Dashed lines indicate mean Arctic (blue) and Pacific (red) d-excess values. Precipitation origin determined using HYSPLIT back-trajectories. Isotope data available at: *http://www.iaea.org/water*.
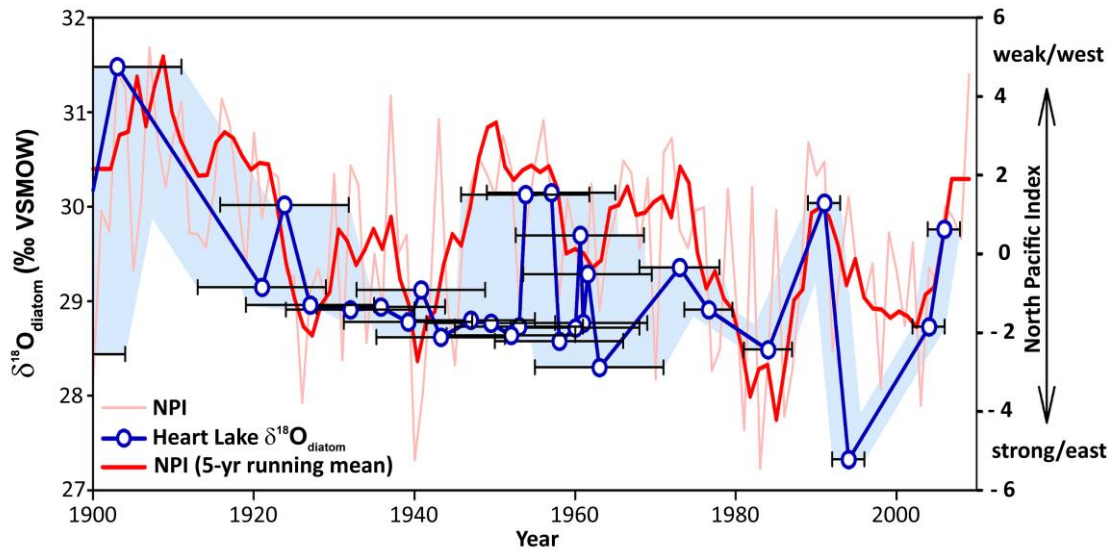
Figure 4. Time series of winter (NDJF) North Pacific Index (NPI) [*Trenberth and Hurrell*, 1994] and $\delta^{18}O_{diatom}$ from Heart Lake. Light red line is the annual NPI time series, dark red is the 5-year running mean. Shaded blue area indicates the age model error range ($\pm$ 0–8 years) for the $\delta^{18}O_{diatom}$ samples, as shown in Table S2. All $\delta^{18}O_{diatom}$ measurements have an analytical precision of $\pm$ 0.1–0.2 ‰ (1σ). Data are listed in Table S3 in Supporting Information.
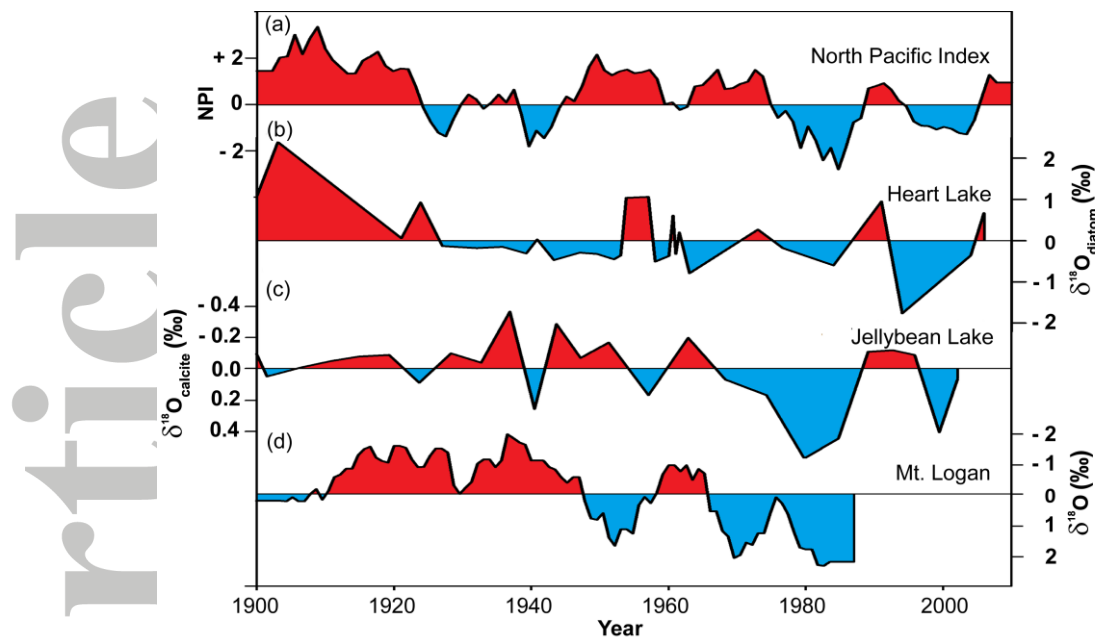
Figure 5. Comparison of **(a)** 20th century North Pacific Index (NPI) [*Trenberth and Hurrell*, 2004] with **(b)** Heart Lake $\delta^{18}O_{diatom}$ (this study) **(c)** Jellybean Lake $\delta^{18}O_{calcite}$ [*Anderson et al.*, 2005) and **(d)** Mt. Logan ice $\delta^{18}O$ [*Moore et al.*, 2002]. Values are expressed as anomalies from the 100 year mean for each record (black lines).